

Ground Antennas in NASA's Deep Space Telecommunications

W. Raftery, S. D. Slobin, C. I. Stelzried, and M. K. Sue

Jet Propulsion Laboratory

California Institute of Technology

4800 Oak Grove Drive

Pasadena, California 91108

ABSTRACT

Ground antennas are the major visible components of NASA's Deep Space Network (DSN). The role, key characteristics, and performance of these antennas in deep space telecommunications are described. The system analyses and tradeoffs to optimize the overall ground-to-spacecraft link and to define future missions are elaborated from an antenna perspective. Overall performance of receiving systems is compared using the widely accepted G/T figure-of-merit, i.e., net antenna gain divided by the operating system noise temperature. Performance of past, present, and future antennas and receiving systems is discussed, including the planned development of a worldwide network of 34-meter diameter beam-waveguide antennas. The need for multi-frequency operation, presently at S- and X-bands, and in the future at Ka-band, is discussed. The resulting requirements placed on antenna technology are highlighted. Beam-waveguide antenna performance to further improve performance and operational advantages is discussed.

This work was performed at the Jet Propulsion Laboratory, California Institute of Technology, under a contract with the National Aeronautics and Space Administration.

1.0 INTRODUCTION

The tenuous link between Earth and those spacecraft that explore our solar system relies heavily on ground antennas [1]. Indeed, antennas are often used to symbolize the Earth-based end of the deep space telecommunication link because of their physically dominating presence at ground stations [2].

The large aperture size is of course associated with high gain, a prerequisite for the signal-starved deep space telecommunications environment. ("Deep space" is defined as a distance beyond the orbit of the Moon,) Ground stations have evolved considerably since the first missions that went beyond earth-orbit, e.g., the U.S. Pioneer 3 and 4 lunar probes in 1958 and 1959 [3]. Station complexity and performance have increased significantly to meet more ambitious, and challenging mission goals, e.g., higher telemetry rates for increased science return, increased operating distances to enable "tours" of our solar system and beyond, and more precise navigation to permit exact spacecraft maneuvers such as gravity-assisted flybys and orbit insertion at distant planets.

Ground antennas are a key part of the complete microwave receiving system that includes feeds, low noise amplifiers, cryogenics, and other microwave components. The receiving systems used in the early days of the American space program were configured with 26-meter diameter antennas operating at 960 MHz (L-band) with receiver noise temperatures of approximately 1500 K [4]. The corresponding spacecraft transmitter power was 0.2 W, which allowed a maximum communications range of approximately 2×10^6 km (only 5 times the distance to the moon), or 0.013 AU (One AU [Astronomical Unit] is equal to 1.5×10^8 km, i.e., the mean distance between the Earth and the Sun.) While 26-m antennas are still in use, primarily for near-Earth communications, the burden of deep space telecommunications is borne by larger antennas, 34 to 70 meters in diameter.

Figures 1 and 2 show a 70-meter diameter antenna and a 34-meter diameter high-efficiency (HEF) antenna presently used in the NASA Deep Space Network (DSN), both of which operate at L-band (1.7 GHz, 70-meter only), S-band (2.3 GHz) and X-band (8.4 GHz). Figure 3 shows a 34-meter diameter beam-

waveguide (BWG) R&D antenna located at the Goldstone Deep Space Communication Complex (GDSCC), which is the prototype of a new series of antennas to be implemented in the DSN, which will operate at S-, X-, and Ka-(32 GHz)-bands [5-8]. The 34-meter BWG antenna is similar to the HEF antenna in many respects, but with the addition of a multi-mirror beam waveguide system below the main reflector surface (Figure 4). S- and X-bands are the current frequencies used in U.S. missions; however an L-band capability at 1.7 GHz is still maintained [9, 10], for possible future support of European Space Agency missions. Operation at 32 GHz is on the horizon [11, 12], and will be discussed later.

In the DSN, ground antenna gains have improved significantly over time due to increases in both antenna size and operating frequency. Equally dramatic is the reduction in system noise temperature, decreasing from 1500 K at L-band in 1958 to less than 16 K at S-band today. System noise is of great importance to the deep space link designer. The major sources of noise are cosmic, galactic, atmospheric, microwave, and electronic. Optimizing a deep space telecommunications link almost always translates into maximizing the ground-received signal-to-noise ratio. This necessitates system-level ground/space trade-offs to be performed, as well as specific subsystem trades within the spacecraft and within the ground stations. In defining the overall link performance, the governing free-space transmission equations are used to construct a link performance budget or table. In analyzing this link, a widely-used figure-of-merit is often employed, i.e., receiving antenna gain divided by the system noise temperature -- G/T . The utility of this figure is readily appreciated for mission designs where the spacecraft (or satellite) antenna aperture and transmitted RF power are kept constant. In this situation, the G/T of different antenna systems allows performance advantages to be determined directly,

Antenna gain has increased by about 28 dB principally through increased aperture, and system noise temperature has decreased by about 20 dB, for a net performance increase from ground-based systems alone of nearly 50 dB at X-band. In parallel, spacecraft improvements such as larger antenna and higher

transmitter power, coupled with advances in coding (which require simultaneous spacecraft and ground improvements) have improved the total NASA deep space communications capability by at least an additional 50 dB. In the next 20 years, an additional 20 dB improvement is expected to be achieved from both ground and spacecraft improvements.

The pursuit of higher G/T has led to the construction of numerous 64 and 70-meter diameter antennas throughout the world [13] and the development of maser low noise amplifiers [14]. These masers are cooled to temperatures below 5K and typically reside in feed cones, located at the antenna's secondary (cassegrain) focus between the main- and sub-reflector surfaces (Figures 1 and 2). These feed cones, which are typically about 2.5m in diameter and 6m tall, house the feedhorn, waveguide, and low noise amplifiers for the antenna. While it is undeniable that large antenna aperture is essential, the practical implications of the maintenance and operation of structures as large or larger than 70-meter antennas have necessitated close investigation. Arraying of smaller antennas in the 30-40-meter size range is an attractive option in terms of antenna investment, ease of construction and maintenance, and operational flexibility. This is possible because of the advances in electronics and digital signal processing, highly stable station equipment, and global networking.

Deep space antennas are operated on five continents in many countries, including the United States, Russia, Australia, the European Community, and Japan. The NASA Deep Space Network (DSN) spans three continents to maximize ecliptic plane visibility. Besides being the largest network of antennas (consisting of three 70m antennas, six 34m antennas, and three 26m antennas), the DSN is also the most sensitive, having very large antennas operating at very low system noise temperatures [15-18]. DSN communication complexes are in the United States at Goldstone, California, in Spain near Madrid, and in Australia near Canberra. In this paper, the role of ground antennas in deep space telecommunications is presented principally in terms of the NASA program.

2.0. DEEP SPACE TELECOMMUNICATIONS CHARACTERISTICS

Deep space telecommunications links consist of an uplink (command) and a downlink (telemetry). This uplink/downlink capability enables the sending of commands to and the receiving of telemetry from distant robotic spacecraft, permitting the collection of valuable scientific data generated by on-board science instruments and of data to monitor the performance of the spacecraft. In addition, these links provide radio metric data to navigate the spacecraft and to support various radio science experiments. The telemetry link poses the greatest challenge to the telecommunications system designers for a number of reasons. Principally, the uplink traffic is significantly less than the downlink traffic. Moreover, the command link also benefits from the very high uplink power (on the order of 100 KW) available from the DSN antennas. This high power capability is not shared by the spacecraft, which is severely resource limited. The limited downlink power and very large communications distances (e. g., 30 AU for Voyager at Neptune encounter, with a round trip light time of 8 hours) present a formidable challenge. Much of the burden to overcome this challenge rests on the DSN ground stations. The following description shows the effect of spacecraft and ground antenna sizes, and operating frequency on telecommunications link performance.

The signal power from a spacecraft, received at a ground antenna, is given by [19]

$$P_r = P_t G_t A_r / (4\pi r^2) \quad (1)$$

where P_t = spacecraft transmitter power

G_t = transmitting antenna gain

A_r = receiving (ground) antenna effective area

r = distance from spacecraft to ground antenna

The transmitting antenna effective gain can be expressed as

$$G_t = 4\pi A_t / \lambda^2 \quad (2)$$

where A_t = effective area of transmitting antenna

λ = wavelength

Rewriting Eqn. (1), in different formulation

$$P_r = P_t \pi D_t^2 A_r / (4\lambda^2 r^2) \quad (3)$$

$$= P_t A_t A_r / (\lambda^2 r^2) \quad (4)$$

$$= P_t G_t G_r / (4\pi r / \lambda)^2 \quad (5)$$

where:

D_t = effective diameter of transmitting (spacecraft) antenna

A_t, A_r = effective areas of transmitting and receiving antennas

G_t, G_r = gains of transmitting and receiving antennas

For a given acceptable received power at a particular wavelength, a tradeoff can be made between the sizes of the spacecraft and ground antennas. If a smaller ground antenna is desired (due to cost or operational considerations), a larger spacecraft antenna or greater transmitter power is required. This burdens the spacecraft with weight, power, and pointing problems. If it is desired to hold spacecraft pointing requirements constant, the quantity λ/D (approximately equal to antenna beamwidth in radians) must be held constant. It follows that some advantage on the spacecraft may be achieved by simultaneously reducing antenna diameter and reducing wavelength (increasing the frequency). This lowers the weight of a spacecraft, while maintaining pointing requirements constant. However, if spacecraft and ground antenna pointing technology improve, antenna diameter can be maintained even as frequency is increased, i.e., the gains of transmitting and receiving antennas both increase.

For a design decision to fix spacecraft weight, power, antenna size, and consumables, in addition to all other things being equal, the performance of a telecommunications link improves dramatically as the operating wavelength is decreased (operating frequency increased), thus in the DSN, the trend has been to higher and higher frequencies, beginning with L-band (960 MHz) in 1958, S-band (2.3 GHz) in 1964, and X-band (8.42 GHz) in 1970. Presently a new series of 34-meter diameter beam waveguide antennas capable of operating at Ka-band (32 GHz) have been designed to supplement existing 34-meter cassegrain-type antennas operating at S- and X-bands. The beam waveguide antennas operate in the cassegrainian mode, with the microwave focus transferred to a pedestal room located below the antenna (Figure 4 and [5-8]). As discussed above, a telecom link using these antennas at Ka-band (and appropriate spacecraft hardware) would theoretically have an 11.6 dB $[10 \log((32/8.42)^2)]$ signal-to-noise ratio (SNR) advantage over an X-band system using the same size antennas and identical spacecraft power (Eqn. 4). (The SNR is directly related to the G/T of the receiving station.) However, atmospheric attenuation and noise temperature contribution in particular (among several other losses) somewhat reduce the overall Ka-band performance advantage compared to lower frequencies.

Numerous sources of loss conspire to reduce the received power and SNR at the ground antenna, among these being transmitting and receiving antenna pointing loss, atmospheric loss, polarization loss, and various other system losses. Typically, large ground-based antennas also have structural (main reflector) deformation which causes a varying efficiency over the operating range of elevation. This effect can be significant for large antennas operating at frequencies above 20 GHz.

3.0. KEY PARAMETERS AFFECTING THE G/T OF THE ANTENNA SYSTEM

3.1 Antenna Gain

Many parameters ~~have an effect~~ on achievable antenna gain, including reflector size, reflector surface roughness, gravity deformation, atmospheric effects, antenna system losses, antenna pointing accuracy, and frequency of operation. Figure 5 shows net antenna gain vs. elevation angle for six typical DSN antenna/frequency combinations at the Goldstone DSCC under average clear weather conditions. Of particular note is the 22 dB range from the case of a 34 meter antenna (high efficiency, HEF) operating at S-band to that of a different type 34-meter antenna (future BWG) operating at Ka-band. Note also that the 34-meter BWG antenna at Ka-band has about 4 dB more peak gain than a 70-meter antenna operating at X-band,

Although DSN antenna main reflector structures are not specifically designed to deform homologously, i.e., to maintain a perfect paraboloidal or shaped contour during gravity-induced deformation, there still exists a best-fit geometrical surface anti focus for the antenna as a function of elevation angle. It is thus necessary to refocus the subreflector both laterally and axially to retrieve the gain [20]. To the extent that perfect reflector shape and perfect focussing cannot be maintained, there will exist some gain roll-off with elevation angle for every DSN antenna. The effect is insignificant for small, stiff antennas operating at S-band; however the effect is easily seen on a 70 meter antenna operating at X-band, and amounts to as much as 0.5 dB due to structural effects alone. The lateral movement of the subreflector causes a pointing change, thus a correction to predicted pointing (as a function of subreflector position) is made so as to accurately track a spacecraft. This pointing correction, known as "squint correction", is typically less than about 0.2 degrees. The correction is required, however, because of the very narrow beamwidths of the DSN antennas (e. g., 0.031 degrees for the 70m antenna operating at X-band),

Large reflectors typically consist of small panels that are mounted on the main reflector support structure. These panels are adjusted individually in the DSN, usually by means of microwave holography using Ku-band (12 GHz) geostationary satellite beacons [21]. This technique can provide an accurate reflector surface to maximize antenna efficiency, at least for the elevation angle (i. e., the rigging angle) at which

the panels are set. The achievable total reflector surface accuracy, which impacts the peak antenna efficiency, is influenced by the resolution of holography, the surface accuracy of the individual panels, and the finite step size of panel adjustment. The total gain reduction due to main reflector surface inaccuracy can be approximated by the root-sum-squared (rss) effect of structural deformation, panel setting inaccuracy, and panel manufacturing imprecision,

For a typical DSN antenna, e.g., a 34-meter HEF (high-efficiency) antenna at X-band, certain antenna-specific losses reduce the peak vacuum gain of the antenna at the rigging angle, typically near 45 degrees elevation. These losses which are given in Table 1 reduce the peak aperture efficiency to 74.5%. Although at X-band the main reflector rss surface roughness (which includes antenna panel manufacturing and setting errors) of 0.55 mm contributes only 0.16 dB to gain loss, at a much higher frequency such as Ka-band (32 GHz) this same roughness will contribute 2.14 dB.

Operational 34m Ka-band BWG antennas are being constructed at the DSN sites which will have panels designed to have a surface accuracy of 0.13 mm (0.005 inch). At the nominal rigging angle of 45 degrees, the panels can be set, with some effort, to yield an expected total surface accuracy of 0.35 mm to the main reflector, using satellite holography. This would cause a Ka-band gain loss at the rigging angle of 1.1 dB, due to an rss surface roughness (panel setting plus manufacturing) of 0.37 mm. A long-term goal is to reduce the surface roughness at the rigging angle to less than 0.25 mm, which would limit the Ka-band gain loss to less than 0.45 dB. Structural deformation away from the rigging angle will of course cause additional loss.

Atmospheric effects reduce the G/T performance of a receiving station in two ways: signal attenuation and increased system noise temperature. For low noise receiving systems such as in the DSN, the effect of increased system noise temperature is more pronounced (see Section 3.2). Atmospheric attenuation has

the effect of reducing the useful gain of an antenna, and is a function of the operating frequency, weather condition, station location and elevation angle. Of the three frequency bands allocated for deep space communications (S-, X-, and Ka-bands), atmospheric attenuation is most severe at Ka-band and least at S-band. To assess the atmospheric effects, statistical models have been developed to characterize the amount of atmospheric attenuation for given a weather condition, station location, operating frequency, and elevation angle.

Table 2 gives atmospheric attenuation at zenith for various weather conditions at the Goldstone (GSTN) and overseas (Canberra/Madrid) DSN antenna locations. As both the Canberra and Madrid locations have similar weather (about 6 times the yearly rainfall of Goldstone), the weather effects are given as a combined model (CAN/MAD),

Weather cumulative distribution (CD) refers to that weather condition which is NOT exceeded a certain percentage of the time. e.g., 90% weather represents a condition (atmospheric noise temperature or attenuation) which NOT exceeded 90% of the time. In other words, 90% of the time, a particular weather effect is less than or equal to a specific value. Conversely, 90% weather IS exceeded 10% of the time. Qualitatively, 0% is the lowest-loss atmosphere, 25% weather is "average clear", 50% weather is clear and humid, and 90% weather may be considered to be very cloudy, but with no rain. As can be seen in Table 2, atmospheric attenuation is much more severe at Canberra and Madrid than at Goldstone. Elevation angle modelling of attenuation is done using a "flat-earth model" (valid above about 6 degrees), which can be described by the following equation:

$$A(\theta) = A_{zen} / \sin(\theta), \text{ dB} \quad (6)$$

where A_{zen} = zenith attenuation in Table 2

θ = elevation angle

Figure 6 shows X-band effective gain curves for the DSN 34-meter HEF antenna at Goldstone, for conditions of vacuum, 0%, 50%, and 90% weather. (The effective gain of the same type of antenna is lower for Canberra and Madrid, due to larger atmospheric attenuation.) The vacuum curve shows a structural deformation gain loss of about 0.2 dB at high and low elevation angles.

3.2, Noise Temperature

The primary sources of receiving system noise temperature are microwave amplifier, waveguide and horn, antenna spillover and scattering, atmospheric emission, cosmic background, anti galactic noise. For a typical DSN antenna (e. g., a 34-meter HEF antenna operating at X-band), the total system noise temperature under average clear sky conditions at zenith is less than 20 Kelvins. The noise components are given in Table 3 for the Goldstone site.

At 10 degrees elevation angle, for example, the total atmospheric contribution at the Goldstone site becomes about 12.5 K (5.76 air masses), the rear spillover decreases to 0.2 K, the forward spillover increases to 1.0 K, and the quadripod scatter increases to 4.7 K. The net result is a total system noise temperature of 32.8 K. Note that tipping the antenna from zenith to 10 degrees elevation increases the system noise temperature by 2.2 dB ($10 \log (32.8/19.7)$). The system noise temperatures for the overseas sites are slightly higher than for the Goldstone site under clear skies, but are higher under adverse weather conditions due to a larger atmospheric noise contribution.

Clearly, atmospheric noise at low elevation angles can be a significant, if not major contributor to total system noise temperature. This severely limits the choice of usable frequencies for deep space communication. Because of the resonance effects of water vapor and oxygen in the microwave spectrum, reliable communications under clear sky conditions are possible only away from the water vapor absorption band at 18-26 GHz and the oxygen bands at 50 to 70 GHz and 110 to 130 GHz. The usable regions are

thus 1-18 GHz, a "window" from about 30-34 GHz, and another window from about 85-105 GHz. Under adverse weather conditions (clouds and rain, whose effects vary approximately as frequency-squared), noise temperature is raised significantly at all frequencies, 1 able 4 gives zenith atmospheric noise temperature contributions (based on actual measurements) at the DSN Deep Space Communications Complexes, at the three primary DSN communications frequencies of S-Band, X-band, and Ka-band. The Goldstone location in the Mojave Desert has generally benign weather conditions, and thus is ideal for communications which are limited by weather effects. At the overseas locations of Canberra and Madrid, weather effects are considerably worse, Attenuation and noise temperature increases above nominal clear sky conditions are typically triple those at Goldstone.

It is seen in 1 able 4 that at S-band there is little change of noise temperature effect as a function of weather CD, and the DSN experiences virtually no weather-related problems at this frequency. At Ka-band, however, where water vapor and liquid water (clouds and rain) have large effects, low elevation angle noise temperature increases of 50K above nominal clear-sky conditions will be experienced at least 10 percent of the time, especially at overseas sites,

As an example of the atmospheric noise temperature effect on the G/T of low noise receiving systems, a 0.1 dB atmospheric attenuation increase has a 0.1 dB effect on effective antenna gain, but a 6K effect on system noise temperature, thus, the net effect on G/T (for a 20K system) is $0.1 + 10 \log (.26/20)$, or a decrease of 1.24 dB.

Figure 7 presents the 34-meter HEF antenna X-band system noise temperatures versus elevation angle for Goldstone. Shown are the vacuum noise temperature increase due to spillover effects only, and curves including 0%, 50%, and 90% weather.

3.3. Antenna pointing

Antenna pointing accuracy is affected by a number of factors, including the size of antenna, operating frequency, and atmospheric effects. Antenna size affects pointing accuracy in two ways: (1) The narrow beamwidth of large antennas requires a very high pointing accuracy in order to minimize pointing loss, and (2) large reflectors suffer from increased wind loading, which further strains the antenna pointing subsystem.

Table 5 illustrates the effect of wind loading on blind pointing performance for the DSN 34-meter diameter antennas with half-power beamwidths of 0.231 degrees at S-band, 0.063 degrees at X-band, and 0.017 degrees at Ka-band.

Atmospheric refraction can also reduce antenna pointing accuracy. Although the amount of refraction for a given atmospheric condition is the same at all microwave frequencies, the errors in refraction modelling cause far more severe effects at Ka-band than X-band. The DSN presently uses real-time surface weather observations at each antenna complex to calculate refraction corrections during tracking operations. Below 20 degrees elevation, the total refraction correction is typically greater than 0.040 degrees. Thus for Ka-band operation, where the antenna beamwidth is less than half this amount, very accurate refraction corrections must be made,

3.4 G/T Performance

Figure 8 shows the net G/T performance of DSN 34-meter and 70-meter diameter antennas operating at S-, X-, and Ka-bands. The gain values used in these curves are those shown in Figure 5. It is seen that for average clear (CD = 0.25) weather conditions at Goldstone, a 34-meter beam waveguide antenna operating at Ka-band has a significantly greater (as much as 3 dB) G/T than does a 70-meter antenna operating at X-band, except at low elevation angles where atmospheric noise temperature effects at Ka-

band arc large, And, when compared to a 70-meter antenna operating at X-band, Ka-band shows a very large performance advantage at all elevation angles.

3.5 Antenna Arraying

Even the large G/T of a single antenna is sometimes not sufficient to meet the strenuous deep space telecommunications performance requirements. One way to improve the ground station performance is by arraying antennas, where signals received from individual antennas are coherently combined to improve the received SNR [22]. This is equivalent to increasing the effective antenna aperture and consequently the G/T. By arraying one 70m antenna and four 34m antennas, the G/T would increase by about 3 dB over a single 70m antenna under ideal conditions. In practice, the increase is less due to loss in combining signals from the arrayed antennas. This loss is a function of signal strength and combining technique [23]. To increase the effective G/T, antenna arraying has been performed using antennas within a single DSN complex as well as with antennas belonging to other agencies. For example, during Voyager's encounter with Neptune, three DSN antennas at Goldstone (one 70m and two 34m antennas) and the twenty-seven 25m antennas of the VLA (Very Large Array) in New Mexico were arrayed together. Arraying the DSN antennas at Goldstone with the VLA antennas effectively increased the G/T by about 5 dB over that of a single 70m antenna.

3.6 Historical - Evolution of DSN Antenna Systems

Figure 9 shows the increase of receiving system G/T from 1958 to the present time. In 1958 and 1959 when Pioneers 3 and 4 were launched, small antenna size (26 meters), low frequency (0.96 GHz), and high receiver noise (1500K) all conspired to give a very low G/T (approximately 14 dB). Progress was very rapid for the next 10 years, with development of maser low noise amplifiers, increases in frequency to S- and X-bands, and increases of antenna size up to 64 meters in diameter. As a consequence, by 1970,

G/T performance had increased by nearly 46 dB, for a 64-meter antenna operating at X-band. For the Voyager Neptune encounter in 1989, 70-meter antenna size and arraying techniques yielded a maximum G/T of nearly 65 dB. By contrast, a single 34-meter beam waveguide antenna operating at Ka-band (32 GHz) nearly approaches the G/T performance of the multi-antenna arrayed configuration.

4.0. FUTURE DSN ANTENNA SYSTEMS

The worldwide network of DSN S- and X- band antennas has successfully provided reliable telecommunications for many deep space missions. It is expected that X-band will continue to provide substantial telecommunications capability well into the 21st century. But as part of continuous DSN performance improvement and in anticipation of meeting new challenges of future deep space telecommunications, NASA/JPL has begun a program to introduce Ka-band (32 GHz) capability to the DSN. Ka-band is chosen as a vehicle to achieve an even larger G/T to enable or enhance future deep space missions for a number of reasons. Ka-band has the potential, under benign weather conditions, of improving G/T and telemetry performance by about 8 to 10 dB for the same DSN antenna size, spacecraft antenna size and transmitter power (Eqn. 4). Unfortunately, weather effects can be significant at Ka-band, and alternative telecommunications strategies, including spacecraft on-board data storage, are being investigated to mitigate occasional weather-caused difficulties. Ka-band is well suited for low-cost, small missions that are characterized by severe mass and power limitations (e. g., Pluto Flyby mission). It has ample allocated bandwidth to support future missions requiring high data-rates in the 100 MBPS range. In addition, it will significantly improve radio metric data and enhance radio science experiments. A multi-frequency S-, X- and Ka-band DSN will indeed be a very powerful telecommunications system,

4.1 Ka-band Beam Waveguide Antenna Technology

A dual-frequency (X- and Ka-band) 34m antenna system has been built at the Goldstone R&D station (DSS-13, Figures 3 and 4, and References [6-8]). This system includes cassegrain-type primary and

secondary reflectors, a beam waveguide system, ultra-low noise amplifiers (with the entire feed system cooled in liquid helium), and associated electronics. A primary objective of this R&D station is to demonstrate the feasibility and advantage of Ka-band deep space telecommunications. Additionally, this very versatile R&D antenna is one of several involved in the HRMS (High Resolution Microwave Survey) Project [24], designed to detect signals from extraterrestrial intelligent sources,

There are advantages for developing 34m BWG Ka-band antenna systems instead of building even larger X-band antennas. A 34m Ka-band antenna could potentially achieve a higher G/T than a 70m X-band antenna (Figure 8), and it would alleviate some of the major mechanical and structural problems of the existing 70m antennas. Perhaps more importantly, a 34m BWG antenna system would cost significantly less than a 70m antenna system, by approximately a factor of 4. For the cost of a single 70m station, a subnet of four 34m BWG antenna stations can be built. This subnet would also provide operational advantages, including mechanical reliability, redundancy, and multi-beam capability to support simultaneous tracking of up to four spacecraft, or a fewer number in an arrayed configuration of the ground antennas.

To achieve a high G/T, beam-waveguide technology and an ultra-low noise maser amplifier have been employed. The beam waveguide system allows the RF front-end components, including the maser and feedhorn, to be located in a pedestal room (Figure 4) away from the elevation-tipping portion of the antenna structure, which in turn enables these components to be cooled using liquid helium, resulting in an ultra-low noise receiver. Additionally, the configuration flexibility and ease of maintenance of the feed system components is a very strong driver for the beam waveguide type of antenna design. Based on recent measurements at the DSS-13 R&D station, the Ka-band receiver noise temperature is in the range of 5 to 7 K, including waveguide and feedhorn. While the BWG optics system results in slight signal loss and increased system noise temperature, these effects are compensated for by the very low noise receiver and improved availability of several other receiving systems located in the pedestal room.

Operational 34m BWG antenna stations using similar technologies developed for and employed by the R&D station are being built at the three DSN sites in anticipation of the eventual adoption of Ka-band for deep space missions. The performance of these stations based on current design expectation as well as measurements obtained from the R&D station is summarized in Table 6. While a very large G/T has been achieved as shown in the table, ongoing development will provide an even higher G/T to meet future needs.

5.0 Conclusion

DSN antennas have played a vital role in meeting the challenges of deep space telecommunications. Trends in missions currently being planned by NASA and other space agencies suggest numerous, smaller spacecraft. These missions will pose even greater challenges to the telecommunications system designers. Ka-band telecommunications systems clearly have the potential to enhance or even enable some of these missions. The current DSN antenna capabilities form an excellent base for these missions. With planned future improvements and new capabilities, ground antennas will, as in the past, be a key component of these deep space communication links.

TABLE 1

Loss Components which Reduce X-Band Gain of DSN 34-Meter Diameter HFE Antenna

Illumination, spillover, and subreflector blockage	0.35 dB
Waveguide and horn losses	0.12 dB
Subreflector support blockage	0.58 dB
Main reflector roughness	0.16 dB
Other	0.07 dB
	----- ..
Total Loss	1.28 dB

TABLE 2

Atmospheric Attenuation, dB, at Zenith as a Function of Station Location and Frequency Band

Cumulative Distr (CD)	S-Band		X-Band		Ka-Band	
	GST	N CAN/MAD	GSTN	CAN/MAD	GSTN	CAN/MAD
Vacuum	0.0000	0.0000	0.0000	0.0000	0.0000	0.0000
0%	0.0291	0.0307	0.0330	0.0345	0.0830	0.1006
25%	0.0293	0.0312	0.0352	0.0411	0.1150	0.1965
50%	0.0294	0.0315	0.0364	0.0448	0.1324	0.2488
80%	0.0295	0.0320	0.0387	0.0516	0.1654	0.3478
90%	0.0297	0.0326	0.0413	0.0593	0.2023	0.4584

TABLE 3

Noise Temperature Contributors to Zenith System Noise Temperature for
 DSN 34-meter HEF Antenna in Goldstone at X-Band with Average Clear Sky

Receiver and follow-on	4.5 K
Waveguide and horn	7.3 K
Quadripod Scatter	2.4 K
Main reflector anti subreflector losses	0.4 K
Forward spillover	0.0 K
Rear Spillover	0.4 K
Atmosphere	2.2 K
Effective Cosmic Bkgrnd	2.5 K
-----
-total	19.7 K

TABLE 4
 Atmospheric Noise Temperatures at Zenith, K, as a Function of
 Station Location and Frequency Band

Cumulative Distr (CD)	S-Band		X-Band		Ka-Band	
	Gstone	Can/Mad	Gstone	Can/Mad	Gstone	Can/Mad
Vacuum	0.000	0.000	0.000	0.000	().00()	0.000
0%	1.770	1.867	2.006	2.097	5.016	6.070
25%	1.805	1.924	2.170	2.534	7.020	11.888
50%	1.836	1.967	2.276	2.794	8.182	15.172
80%	1.877	2.032	2.458	3.273	10.351	21.321
90%	1.899	2.079	2.633	3.775	12.673	27.897

TABLE 5

Expected 34m Antenna Blind Pointing Accuracy and Pointing Loss in Various Wind Conditions

Wind Speed mph (m/sec)	Mean Pointing Error, mdeg	Pointing Loss at Mean Pointing Error, dB		
		S-Band	X-Band	Ka-Band
<10 (<4.5)	1.67	0.001	0.009	0.123
<20 (<8.9)	3.33	0.003	0.034	0.489
<30 (<13.4)	5.00	0.006	0.076	1.101

TABLE 6

Expected Performance of a 34m BWG antenna at Goldstone, Ka-band, 45-degrees elevation, 90% weather

Vacuum antenna efficiency	49.4 %
Vacuum antenna gain	78.08 dBi
Effective antenna gain	77.79 dBi
System noise temperature	37.75 K
Antenna pointing error	<1.67 mdeg
in 10 mph wind	
Antenna G/T	62.0 dB

REFERENCES

1. J. H. Yuen, ed., Deep Space 1 telecommunications Systems Engineering, Plenum Press, NY, 1983.
2. "The Deep Space Network"; Jet Propulsion Laboratory Publication JPL 400-333, January 1988.
3. N. A. Renzetti, ed., "A History of the Deep Space Network", JPL Technical Report 32-1533, Vol. 1, September 1, 1971.
4. W. F. Corliss, "A History of the Deep Space Network, " NASA CR-151915, May 1, 1976
5. R. C. Clauss and J. G. Smith, "Beam Waveguides in the Deep Space Network", JPL TDA Progress Report 42-88, Vol. Oct-Dec 1986, pp. 174- 182., February 15, 1987.
6. D. A. Bathker, et al, "Beam-Waveguide Antenna Performance Predictions with Comparisons to Experimental Results", IEEE Trans. Microwave Theory Tech., Vol. 40, No. 6, pp. 1274-1285, June 1992.
7. T. Y. Otoshi, et al, "Portable Microwave Test Packages for Beam- Waveguide Antenna Performance Evaluation", IEEE Trans. Microwave Theory Tech., Vol 40, No. 6, pp 1286-1293, June 1992.
8. S. D. Slobin, et al, "Efficiency Measurement Techniques for Calibration of a Prototype 34-Meter-Diameter Beam-Waveguide Antenna at 8.45 and 32 GHz", IEEE Trans. Microwave Theory Tech., Vol 40, No. 6, pp. 1301-1309, June 1992,

9. C. T. Stelzried, et al, "The Venus Balloon Project, " JPL TDA Progress Report 42-85, Vol. Jan-Mar 1986, pp. 191-198, May 15, 1986.
10. C. T. Stelzried, et al, "Halley Comet Missions, " JPL TDA Progress Report 42-87, Vol. Jul-Sep 1986, pp. 240-242, November 15, 1986,
11. R. M. Dickinson, "A Comparison of 8.415-, 32.0-, and 565646-GHz Deep Space Telemetry Links, " JPL Publication 85-71, October 15, 1985.
12. J. W. Layland, et al, "Ka-Band Study-1988, Final Report, JPL Publication 890-212, Document JPL 89-6015, 2/15/89.
13. M. S. Reid, et al, "Low-Noise Microwave Receiving Systems in a Worldwide Network of Large Antennas, " Proceedings of the IEEE, Vol. 61, No. 9, Sept. 1973.
14. R. C. Clauss, J. Bautista, et al, "Ruby Maser Amplifiers...") Proceedings of the IEEE, this issue,
15. N. A. Renzetti and A. L. Berman, "The Deep Space Network - An Instrument for Radio Science Research", JPL Publication 80-93, February 15, 1981.
16. N. A. Renzetti, et al, "The Deep Space Network - A Radio Communications Instrument for Deep Space Exploration", JPL Publication 82-104, July 15, 1983.
17. N. A. Renzetti, et al, "The Deep Space Network - An Instrument for Radio Astronomy Research", JPL publication) 82-68, Rev. 1, Sept. 1, 1988,

18. W. A. Imbriale, "Evolution of the Large Deep Space Network Antennas", IEEE Antennas and Propagation Magazine, Vol. 33, No. 6, pp. 7-19, December 1991.
19. W. C. Lindsey and M. K. Simon, "Telecommunication Systems Engineering," Prentice-Hall, Inc.
20. S. D. Slobin and D. A. Bathker, "DSN 70-m Antenna X-Band Gain, Phase, and Pointing Performance, With Particular Application for Voyager 2 Neptune Encounter, " JPL TDA Progress Report 42-95, Vol. Jul-Sept 1988, pp 237-245, November 15, 1988.
21. D. J. Rochblatt and B. L. Seidel, " Microwave Antenna Holography", IEEE Trans Microwave Theory Tech, Vol 40, No. 6, pp. 1294-1300, June 1992.
22. J. W. Layland and D. W. Brown, "Planning for VLA/DSN Arrayed Support to the Voyager at Neptune, " JPL TDA Progress Report 42-82, Vol. Apr-Jun 1985, pp. 125-135, August 15, 1985.
23. A. Mileant and S. Hinedi, "Overview of Arraying Techniques in the Deep Space Network," JPL TDA Progress Report 42-104, Vol. Oct-Dec 1990, pp. 109-139, February 15, 1991.
24. M. Klein, et al, "Status of NASA SETI Sky Survey Microwave Observing Project", Acts Astronautic, Vol. 26, No. 314, pp. 177-184, 1992,

LIST OF FIGURES

Figure 1 ---- NASA/DSN 70 Meter Antenna at Goldstone Deep Space
Communications Complex

Figure 2 ---- NASA/DSN 34 Meter HEF (High Efficiency) Antenna at
Goldstone Deep Space Communications Complex

Figure 3----34 Meter Prototype NASA/DSN BWG (Beam-waveguide)
R&D Antenna at Goldstone Deep Space Communications
Complex

Figure 4 ---- Cross-Sectional View of L) SS-13 BWG Antenna Showing
Multi-Mirror Beam-waveguide Microwave Optics Design

Figure 5 ---- DSN Antenna Gain Comparison for Various
Antenna/Frequency Configurations, Goldstone,
Average Clear Weather (25% CD)

Figure 6 ---- HEF Antenna Gain at X-band, Goldstone
with 0%, 50%, and 90% Weather Attenuation

Figure 7 ----HEF Antenna System Temperature, Goldstone

with 0%, 50%, and 90% Weather Contributions

Figure 8 --- DSN Antenna G/T Comparison for Various
Antenna/Frequency Configurations, Goldstone,
Average Clear Weather (25% CD)

Figure 9 --- Historical View of DSN Antenna G/T performance

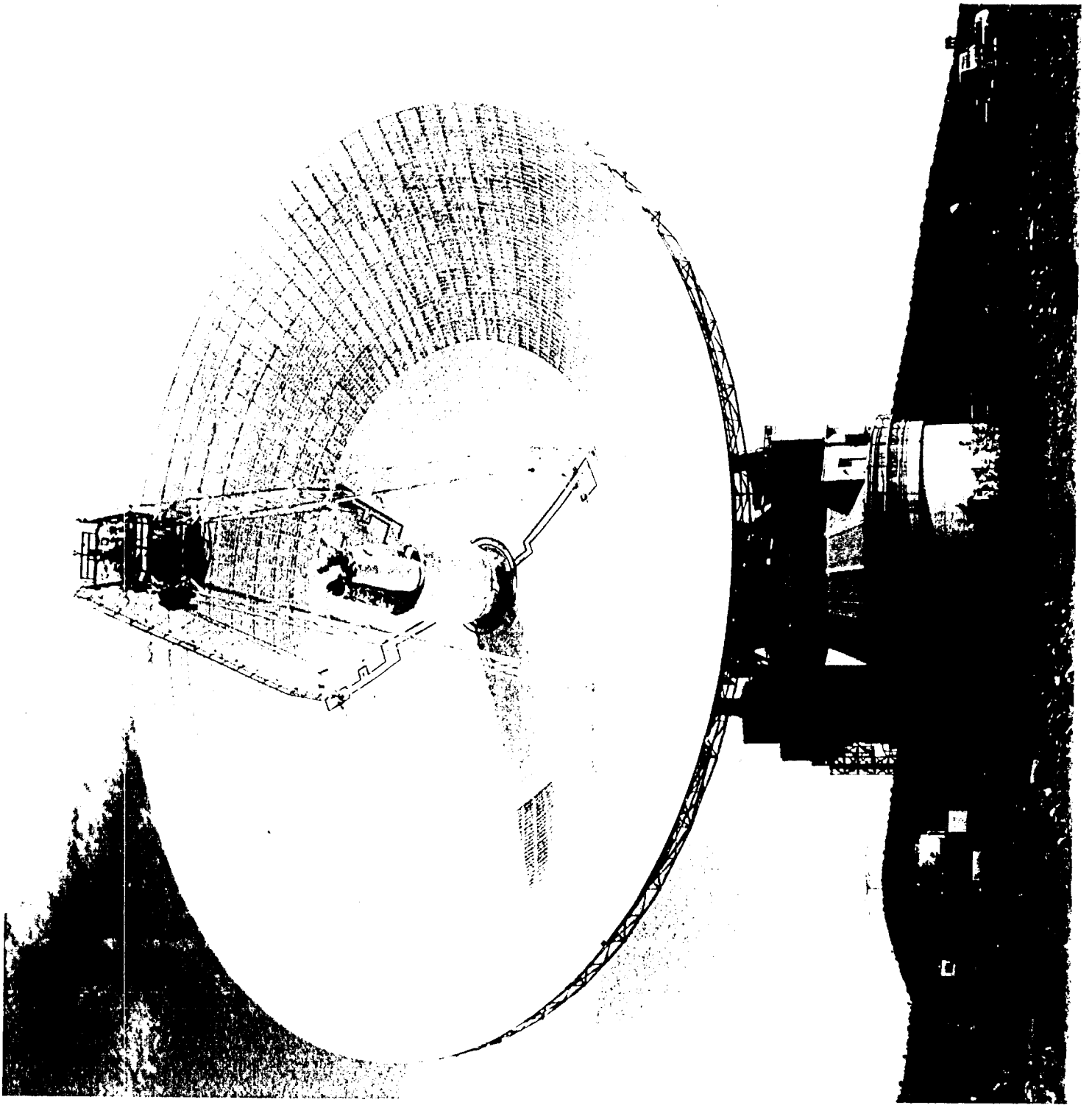


FIGURE 1

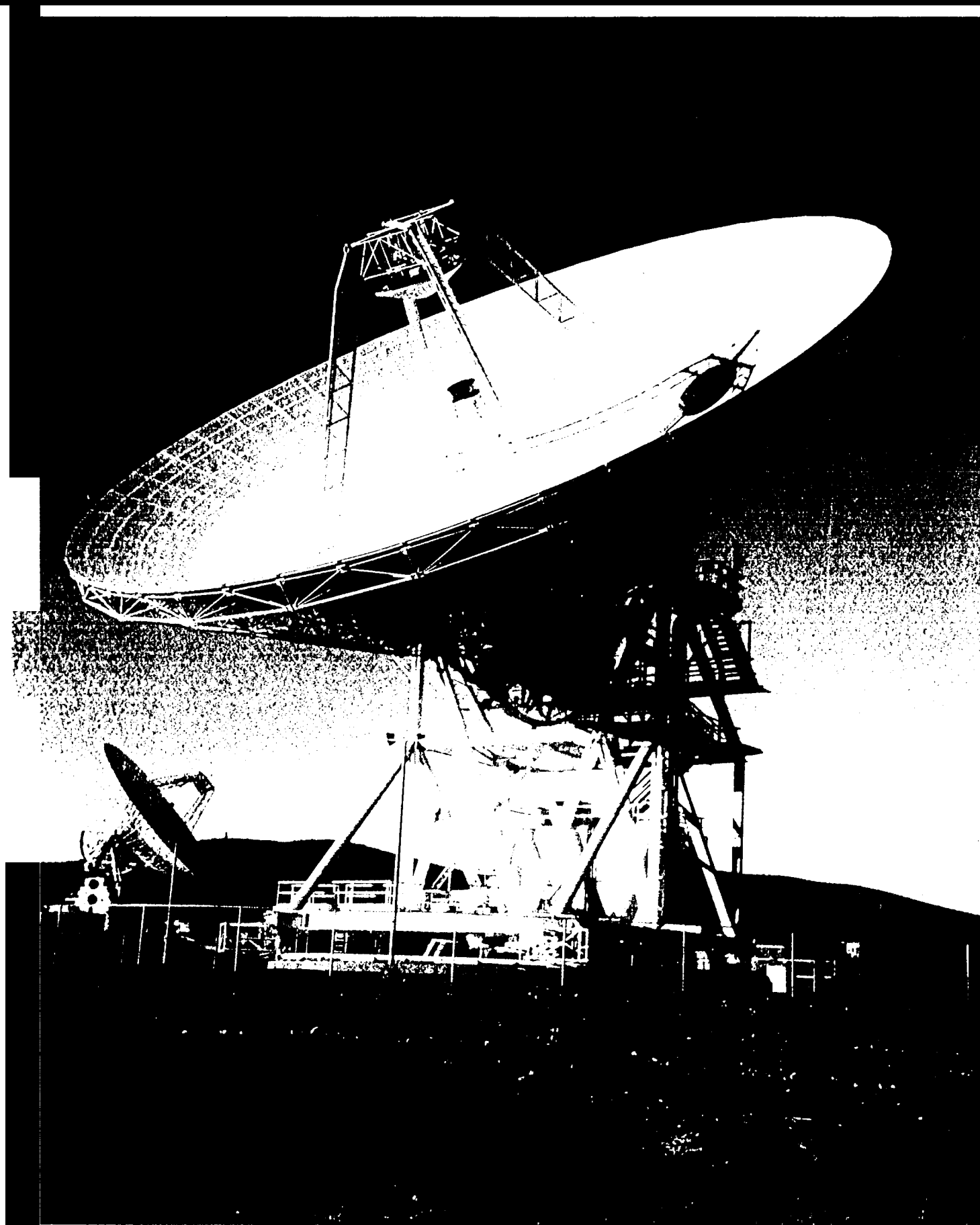


FIGURE 2

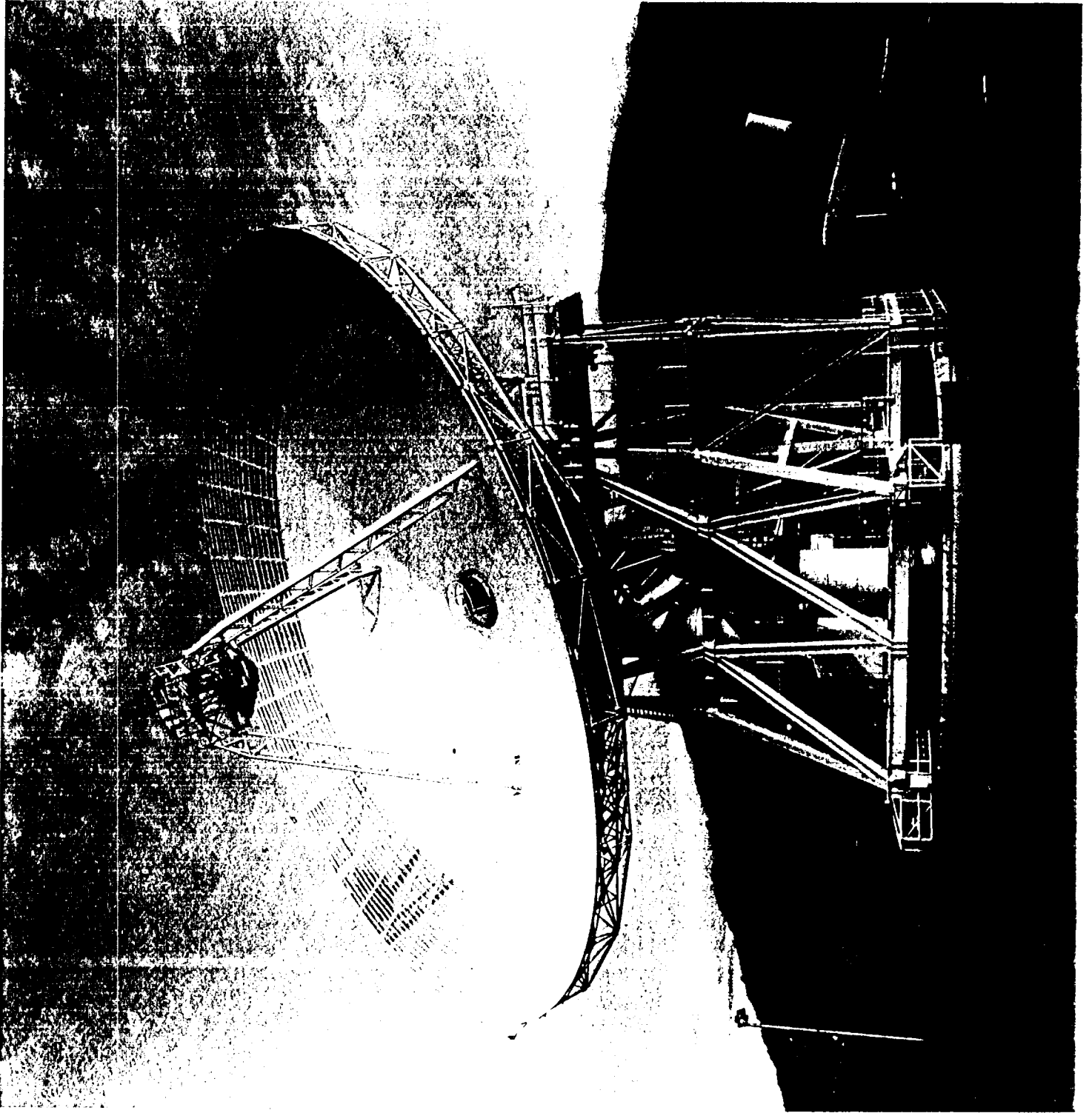
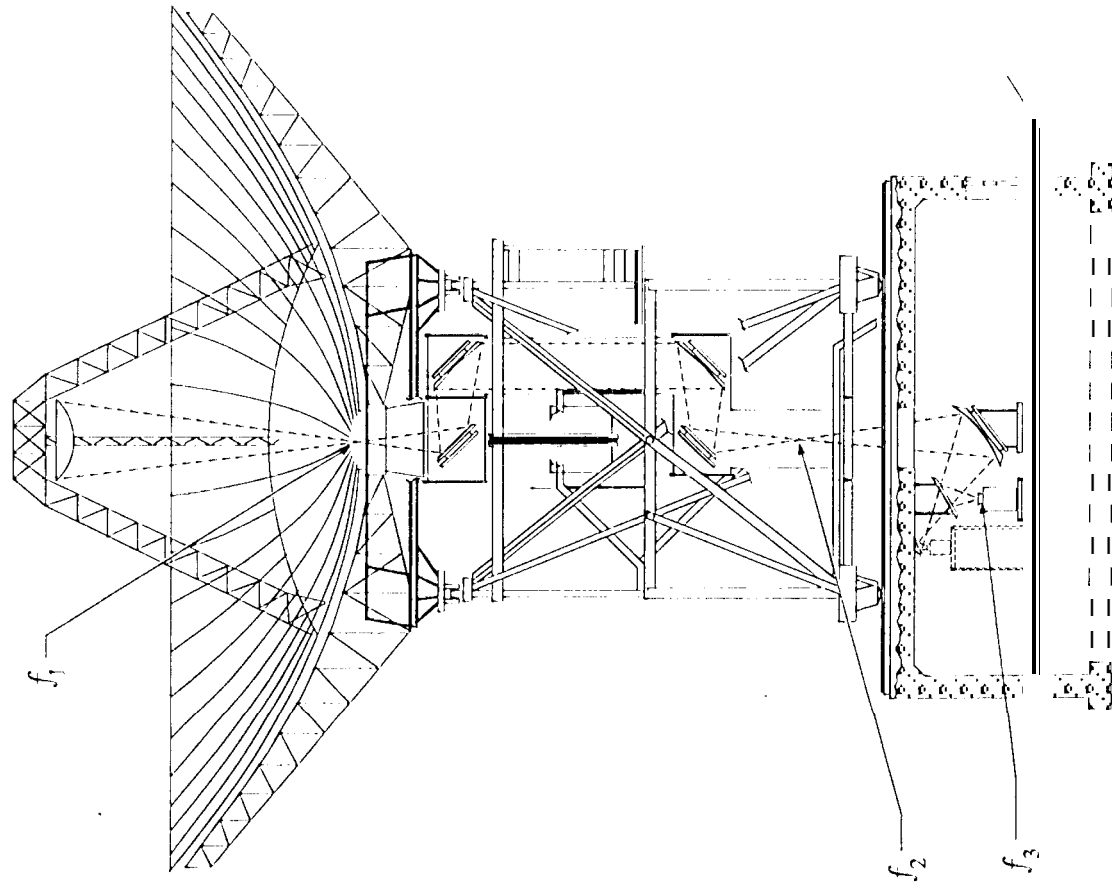


FIGURE 3

SCHEMATIC OF DES 3 BWG ANTENNA



RAFFERTY
FIG. 4

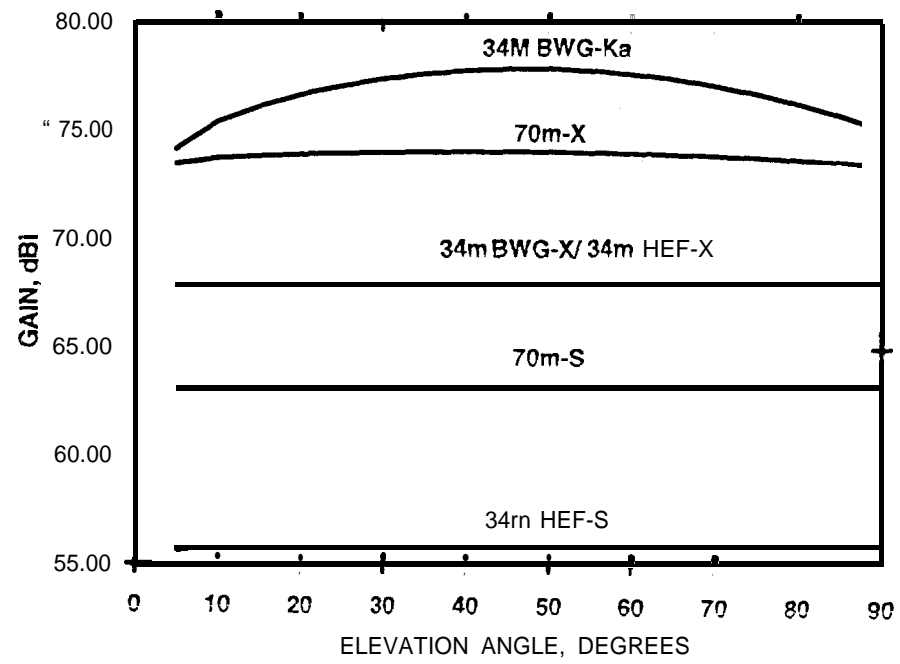


FIGURE 5

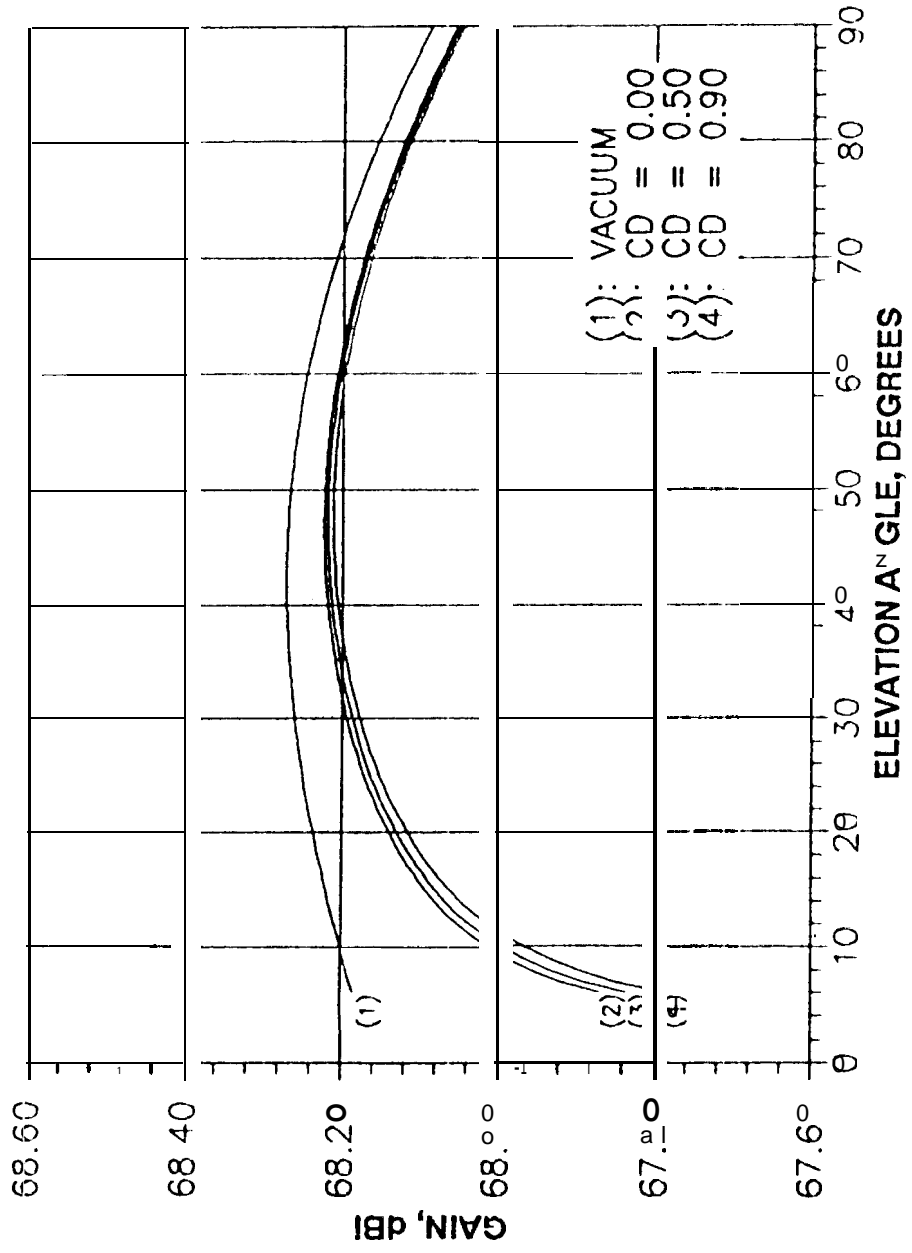


FIGURE 6

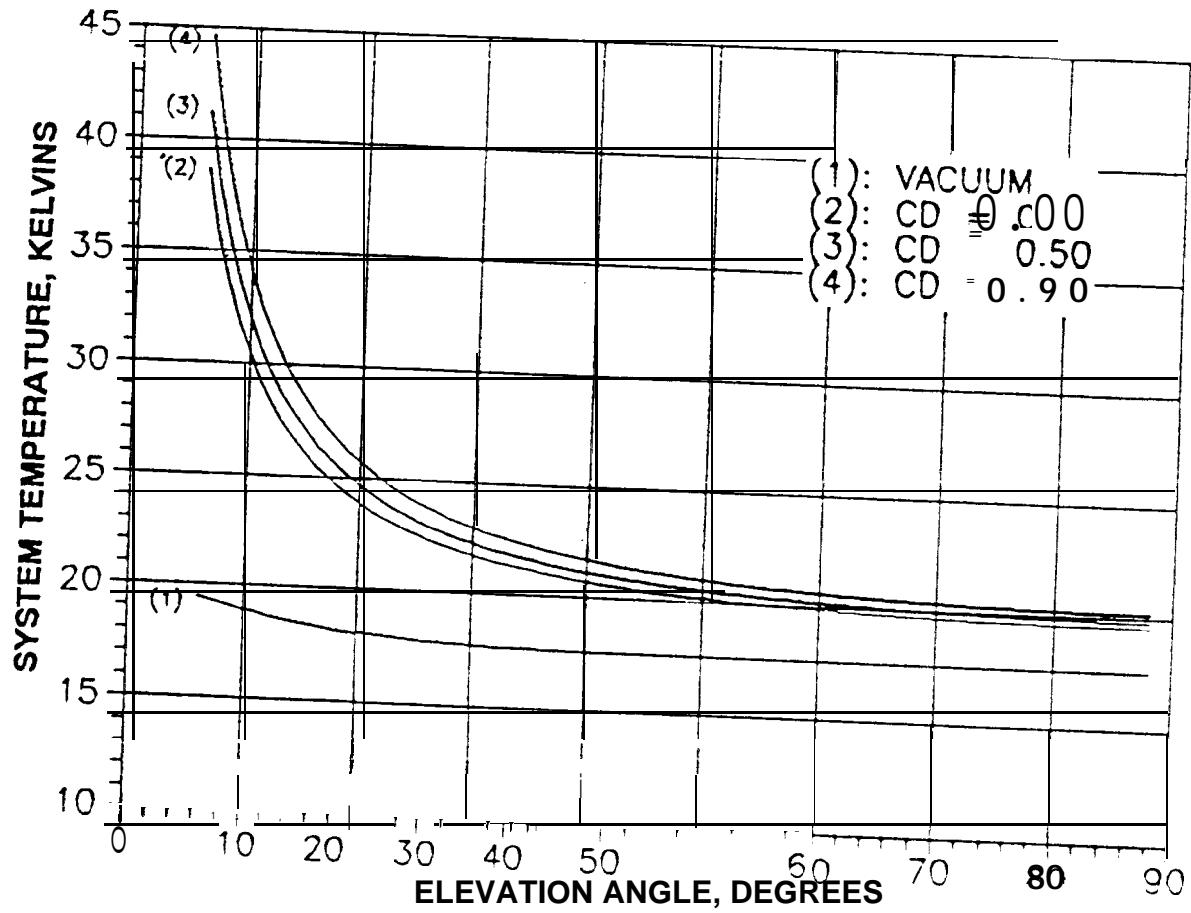


FIGURE 7

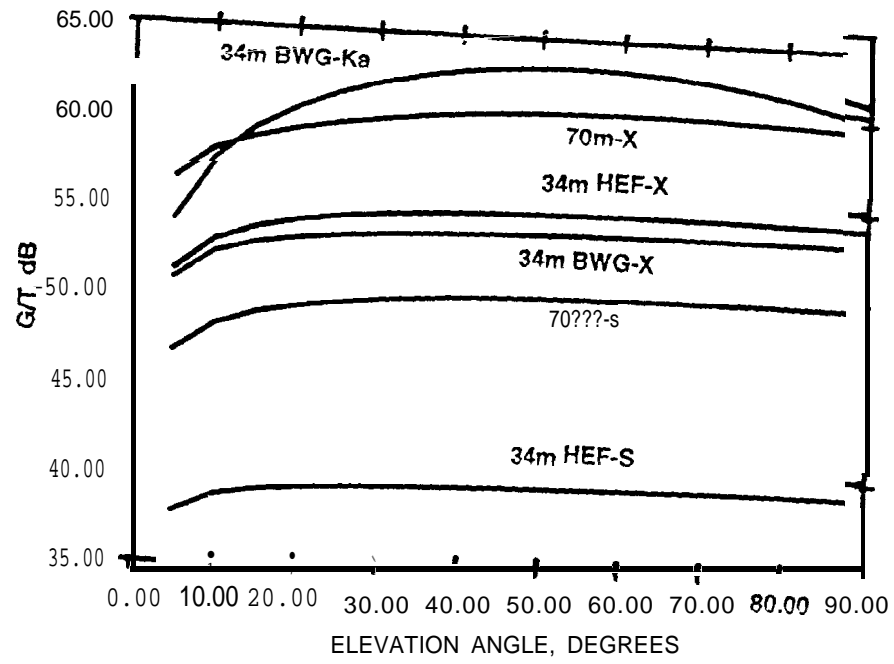
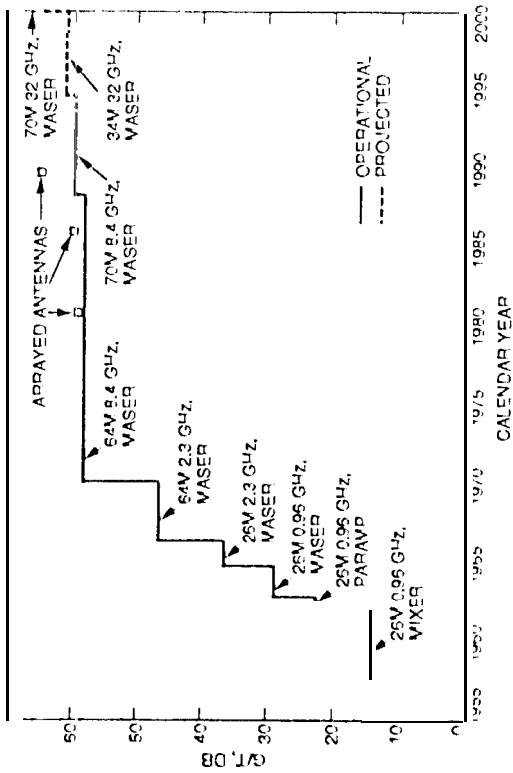


FIGURE 8



MAX WARD

RAFFERTY
F G. 9